frontiers in Oncology

ORIGINAL RESEARCH
published: 02 September 2020
doi: 10.3389/fonc.2020.01770

Identification of Immune-Related Cells and Genes in Tumor Microenvironment of Clear Cell Renal Cell Carcinoma

Bowen Du†, Yulin Zhou†, Xiaoming Yi, Tangliang Zhao, Chaopeng Tang, Tianyi Shen, Kai Zhou, Huixian Wei, Song Xu, Jie Dong*, Le Qu*, Haowei He* and Wenquan Zhou**

Department of Urology, Jinling Hospital, Medical School, Nanjing University, Nanjing, China

Clear cell renal cell carcinoma (ccRCC) is one of the most common tumors in the urinary system. Progression in immunotherapy has provided novel options for the ccRCC treatment. However, the understanding of the ccRCC microenvironment and the potential therapeutic targets in the microenvironment is still unclear. Here, we analyzed the gene expression profile of ccRCC tumors from the Cancer Genome Atlas (TCGA) and calculated the abundance ratios of immune cells for each sample. Then, seven types of immune cells were found to be correlated to overall survival, and 3863 immune-related genes were identified by analyzing differentially expressed genes. We also found that the function of immune-related genes was mainly focused on ligand-receptor binding and signaling pathway transductions. Additionally, we identified 13 hub genes by analyzing the protein-protein interaction network, and seven of them are related to overall survival. Our study not only expands the understanding of fundamental biological features of microenvironment but also provides potential therapeutic targets.

Keywords: ccRCC, tumor microenvironment, immunotherapy, TCGA, hub gene

OPEN ACCESS

Edited by:
Viktor Grünwald,
Essen University Hospital, Germany

Reviewed by:
Jan Hinrich Bräsen,
Hannover Medical School, Germany
Henning Reis,
Essen University Hospital, Germany

****Correspondence:***
Song Xu
songxu1963@gmail.com
Jie Dong
smiledongjie@163.com
Le Qu
septsoul@hotmail.com
Haowei He
hohowell@163.com
Wenquan Zhou
shzwqzsl@163.com

† These authors have contributed equally to this work

Specialty section:
This article was submitted to Genitourinary Oncology, a section of the journal Frontiers in Oncology

Received: *01 May 2020*
Accepted: *07 August 2020*
Published: *02 September 2020*

Citation:
Du B, Zhou Y, Yi X, Zhao T, Tang C, Shen T, Zhou K, Wei H, Xu S, Dong J, Qu L, He H and Zhou W (2020) Identification of Immune-Related Cells and Genes in Tumor Microenvironment of Clear Cell Renal Cell Carcinoma. Front. Oncol. 10:1770. doi: 10.3389/fonc.2020.01770

INTRODUCTION

Kidney cancer is one of the most common cancer in the world (1). Renal cell carcinoma (RCC) accounts for 85–90% of kidney cancer, while clear cell renal cell carcinoma (ccRCC) accounts for about 70–75% of RCC (2–6). ccRCC is frequently characterized by the von Hippel Lindau (VHL) tumor suppressor gene lose or inactivation, which leads to the overexpression of the hypoxia-inducible factor-2α (HIF2α), vascular endothelial growth factor (VEGF), and their downstream kinases (7–9). Multiple tyrosine kinase inhibitors (TKIs) have been developed as novel therapies (10), but the 5-year overall survival rate for advanced ccRCC remains under 30% (11, 12). Thus, it is necessary to develop novel therapies for ccRCC treatment.

The tumor microenvironment has been increasingly studied in the field of cancer immunotherapy in recent years. The tumor microenvironment is the non-cancerous cells and molecules surrounding the tumor cells, which consist of immune cells, blood vessels, adipocytes, mesenchymal stem cells, cancer-associated fibroblasts, and extracellular matrix (13, 14). The tumor microenvironment significantly influences therapeutic response and clinical outcomes through

multiple signaling pathways (15). Thus, a better understanding of tumor microenvironment may help us develop novel therapies for ccRCC treatments.

To explore the immune microenvironment component in the ccRCC tumor and its interaction with the tumor cells, we first screened the survival-related immune cells in the ccRCC microenvironment. Then, we identified the immune-cell-specific genes by analyzing differentially expressed genes. To study the biological function of the immune-specific genes, we also enriched those genes in the Kyoto Encyclopedia of Genes and Genomes (KEGG), and Reactome pathways. Finally, we identified 13 hub genes by studying protein-protein interaction (PPI) networks and found seven genes correlated to overall survival. Our study not only revealed the biological features of the ccRCC microenvironment but also provided a novel view of ccRCC therapies.

MATERIALS AND METHODS

Samples and Data Process

We selected 530 ccRCC patients from the Cancer Genome Atlas (TCGA) dataset and excluded 11 patients owing to the incomplete clinical data. The raw count data were downloaded from the TCGA website[1]. The transcripts per million (TPM) values were calculated with R software as the mRNA level of each gene. The clinical data were downloaded from the cbioportal website[2] and summarized in **Table 1**.

[1]https://portal.gdc.cancer.gov

[2]http://www.cbioportal.org

TABLE 1 | Patient clinical characteristics of The Cancer Genome Atlas cohort.

	Case (No.)	Percent (%)
Gender		
Male	337	64.9
Female	182	35.1
Age		
Median	60	
Range	26–90	
Fuhrman grade		
G1	14	2.7
G2	225	43.4
G3	206	39.7
G4	74	14.3
Stage		
I	261	50.3
II	54	10.4
III	122	23.5
IV	82	15.8
T Stage		
pT1	267	51.4
pT2	66	12.7
pT3	175	33.7
pT4	11	2.1

Identification of Survival-Related Immune Cells

The abundance ratios of 22 types of immune cells were calculated with CIBERSORTx (16). The matrix of TPM values for all samples was uploaded to the CIBERSORTx website[3] as the Mixture file. The LM22 matrix within the software was selected as the Signature gene file. The software was run in relative mode. Batch correction and quantile normalization were not performed in this run. The permutations for significance analysis were set to 100. Then, the Kaplan–Meier analysis was performed to identify the survival-related immune cells with the Survival R package based on the abundance ratio of each cell type. The Log-Rank test was used to analyze the survival data, and the medians of the abundance ratios for cell types were as the cut-off values. The relationship between the abundance ratios of immune cells and the pathological grades and the clinical stages were analyzed with the one-way ANOVA test.

Identification of Immune-Related Genes

We identified the specific genes for each type of the survival-related immune cells by calculating the differentially expressed genes between the high- and low-immuno-infiltrated samples with the median of abundance ratios as the cut-off value. The differentially expressed genes were analyzed with the DEseq2 R package. The genes with $|\log_2(\text{foldchange})| > 1$ and p-value < 0.05 were considered as specific genes for that cell type. The results were visualized with the UpSetR R package.

Enrichment Analysis of Immune-Related Genes

The KEGG enrichment analysis was performed with the enrichKEGG function in the Clusterprofiler R package. The list of gene IDs was used as the input file. The Benjamini-Hochberg method was used to adjust the p-values. The cut-off of p-values was set to 0.05. The Reactome enrichment analysis was performed with the enrichPathway function in the ReactomePA R packages. The list of gene IDs was used as the input file. The parameters were set as follow: pAdjustMethod = "BH," pvalueCutoff = 0.05, minGSSize = 10, and maxGSSize = 500. The enrichment results were visualized with the ggplot2 R package.

Constriction of PPI Network and Identification of Hub Genes

The 933 immune-related protein-coding genes were imported into the STRING database[4]. The results with combined scores over 0.7 were kept and visualized with the Cytoscape software. To identify the hub genes, we clustered the genes within the PPI network with the MCODE plugin of the Cytoscape software using the following parameter: Degree Cutoff = 4, Node Score Cutoff = 0.3, K-core = 2, and Max. Depth = 100. The clusters containing over 40 proteins were used to extract hub genes. The hub genes were obtained with the CytoHubba plugin of the Cytoscape software.

[3]https://cibersortx.stanford.edu

[4]https://string-db.org

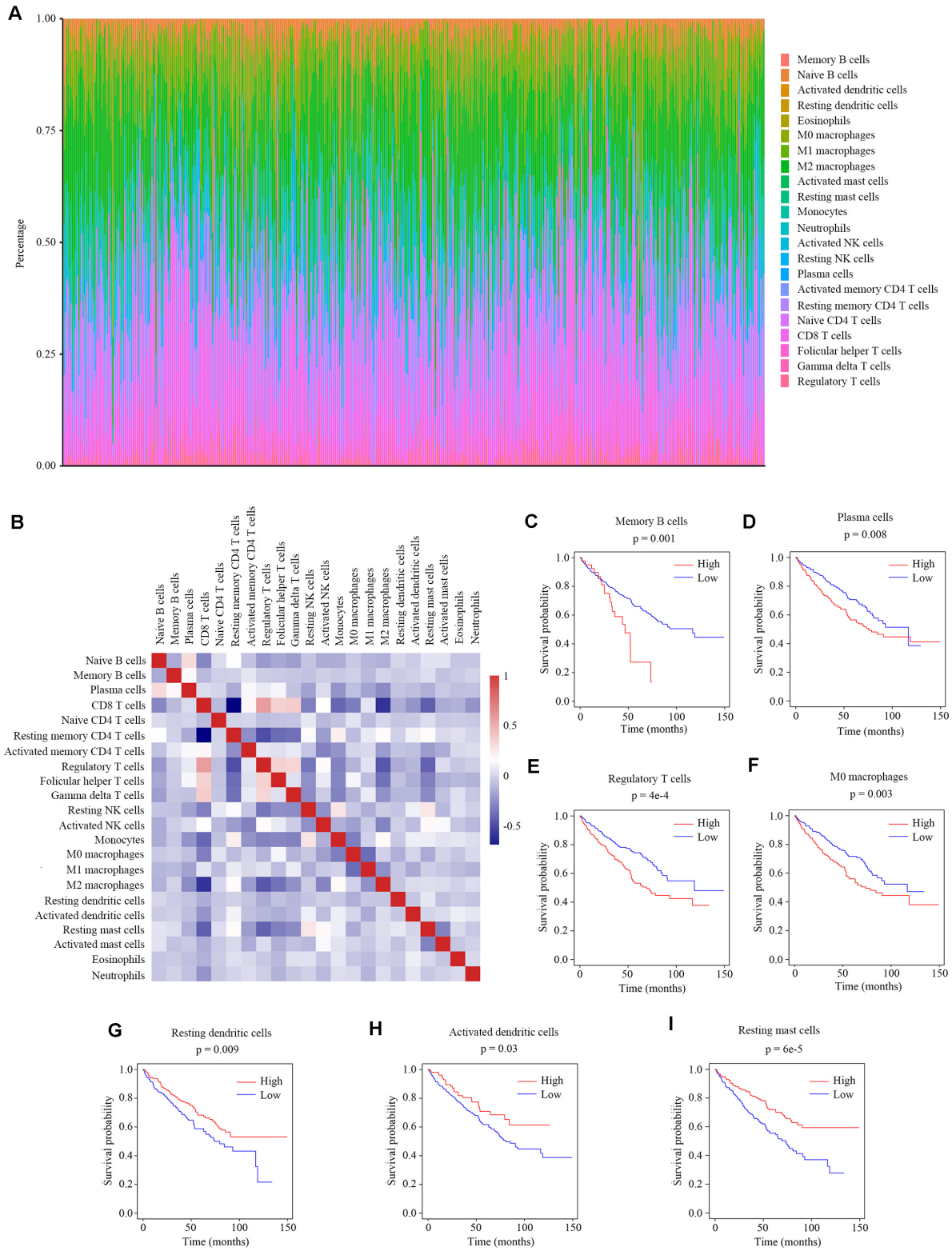

FIGURE 1 | The relationship between the abundance ratios of immune cells and overall survival. **(A)** The abundance ratios of immune cells in the ccRCC samples. Each column represents a sample, and the column height indicates the abundance ratios of the certain immune cells in that sample. **(B)** The correlation coefficient between the abundance ratios of distinct immune cells. **(C–I)** The survival analysis for the abundance ratios of memory B cells, plasma cells, regulatory T cells, M0 macrophages, resting dendritic cells, activated dendritic cells, and resting mast cells.

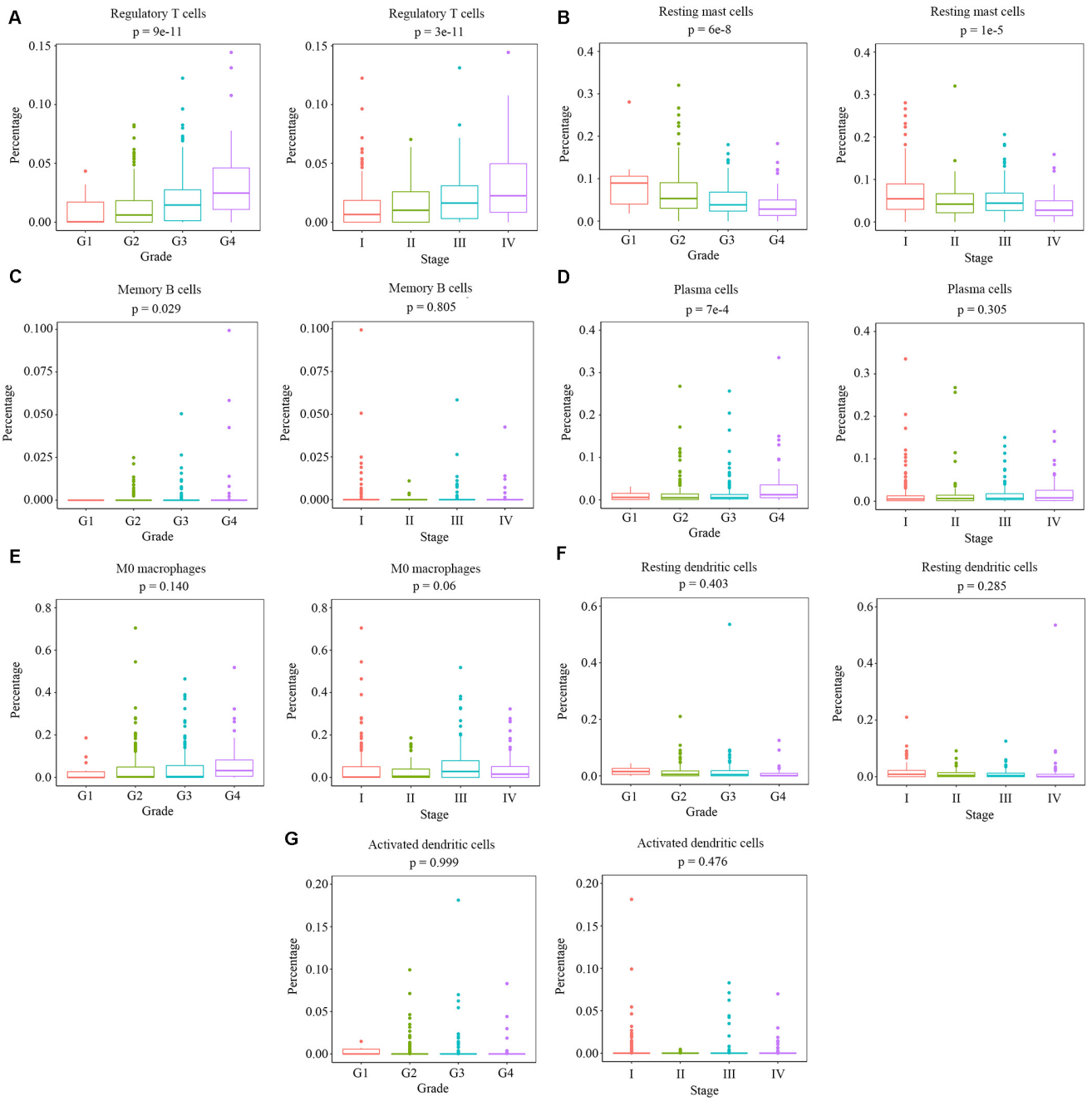

FIGURE 2 | The relationship between the abundance ratios of the immune cells and clinical characteristics. **(A–G)** The abundance ratios of memory B cells, plasma cells, regulatory T cells, M0 macrophages, resting dendritic cells, activated dendritic cells, and resting mast cells in different pathological grades and clinical stages. Data are shown in boxplot format, and the dots represent the outliers.

Relationship Between Immune Infiltration and Hub Genes

The Pearson correlation between the hub genes and all the 22 types of immune cells was calculated, and the result was visualized with the ggplot2 R package. Also, the correlation between the hub genes and the overall survival was calculated with the Log-Rank test.

RESULTS

Identifying Survival-Related Immune Cells

Previous studies have reported the immune infiltration in the ccRCC tumors (17–20). Thus we explored the microenvironment components of ccRCC tumors by calculating the abundance

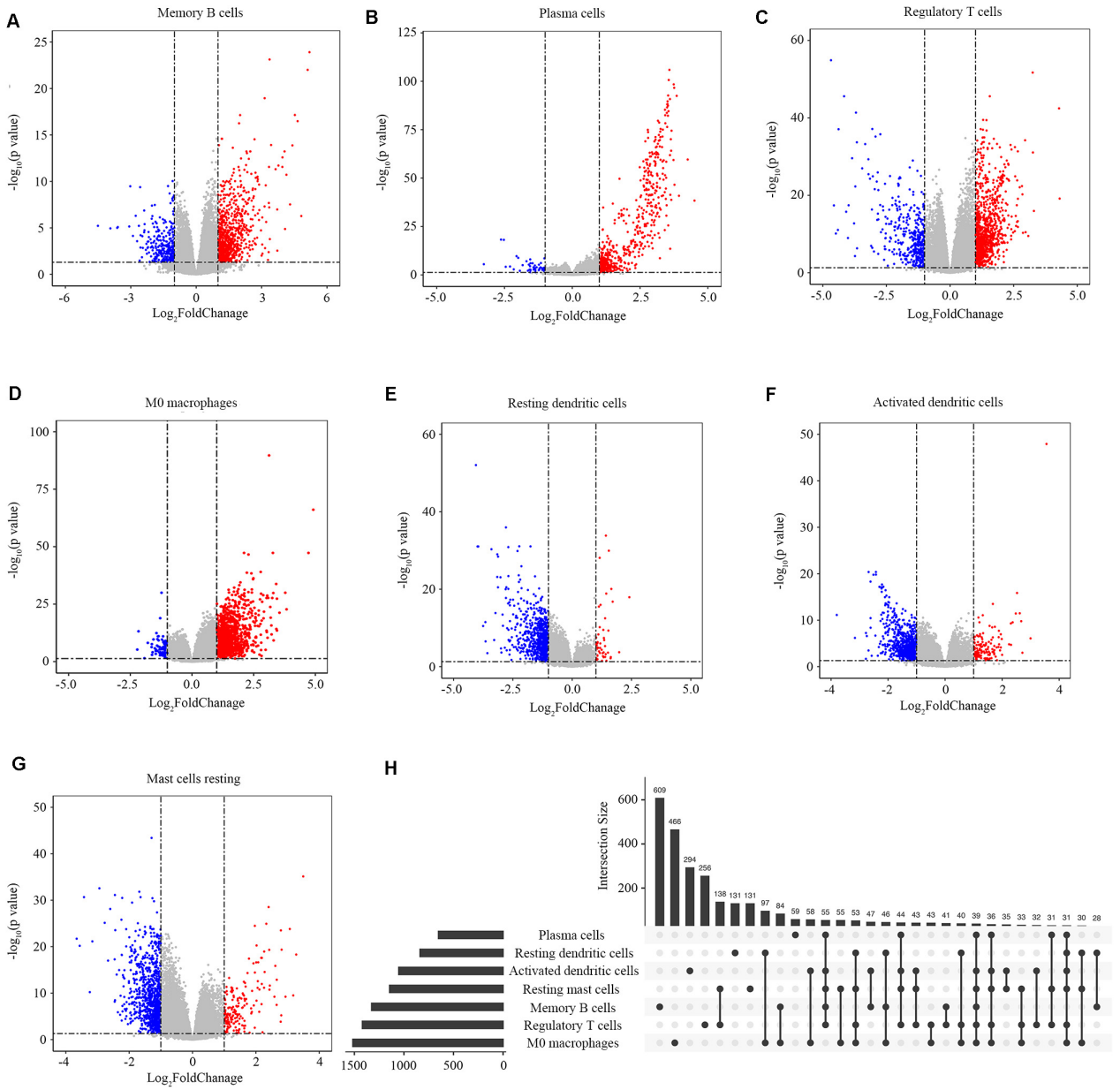

FIGURE 3 | Identification of immune-related genes. **(A–G)** Gene expression profiles related to memory B cells, plasma cells, regulatory T cells, M0 macrophages, resting dendritic cells, activated dendritic cells, and resting mast cells. Data are presented with Volcano plots. The red/blue dots represent the upregulated/downregulated genes according to the criteria: $|\log_2 \text{Foldchange}| > 1$ and adjusted p-value < 0.05. **(H)** The distribution of immune-related genes in the seven types of immune cells. Each black dot represents a set of genes that distributed in one type of immune cell. The numbers on the bar represent the counts of genes in this gene set. The dots connected with a black line represent a common set of genes distributed in more than one type of immune cell.

ratios of 22 types of immune cells with the online software CIBERSORTx (**Figure 1A**). We found the T cells accounted for the most proportion (42.2 ± 14.2%), followed by the macrophages (33.7 ± 11.7%). We also found that the abundance ratios of some types of immune cells were correlated with each other (**Figure 1B**).

The abundance ratios of memory B cells, plasma cells, regulatory T cells, M0 macrophages, resting dendritic cells, activated dendritic cells, and resting mast cells were significantly correlated with the overall survival of ccRCC patients (**Figures 1C–I**). The higher abundance ratios of memory B cells, plasma cells, regulatory T cells, and M0 macrophages identified patients with worse prognosis, while the higher abundance ratios of resting dendritic cells, activated dendritic cells, and resting mast cells identified patients with better prognosis. These seven types of immune cells were considered as survival-related cells and analyzed in further study.

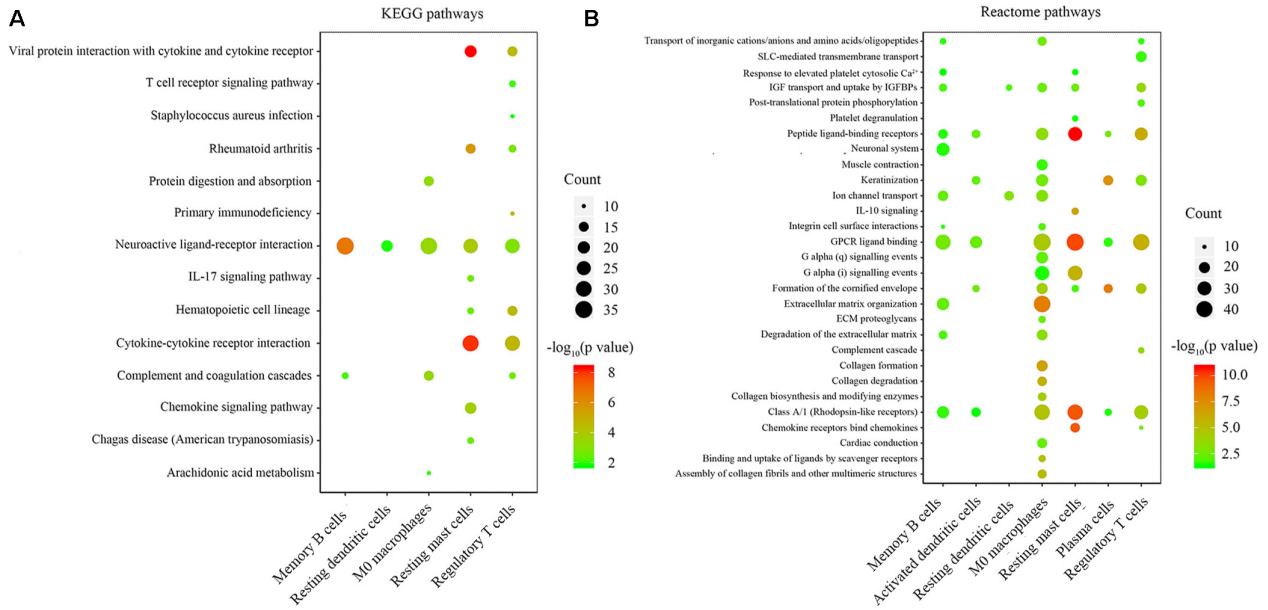

FIGURE 4 | Enrichment analysis of genes related to immune cell infiltration. **(A,B)** the KEGG and Reactome pathway enrichment results of genes involved in each type of immune cells. The color indicates the significance of enrichment results, and the dot size indicates the count of genes enriched for each result.

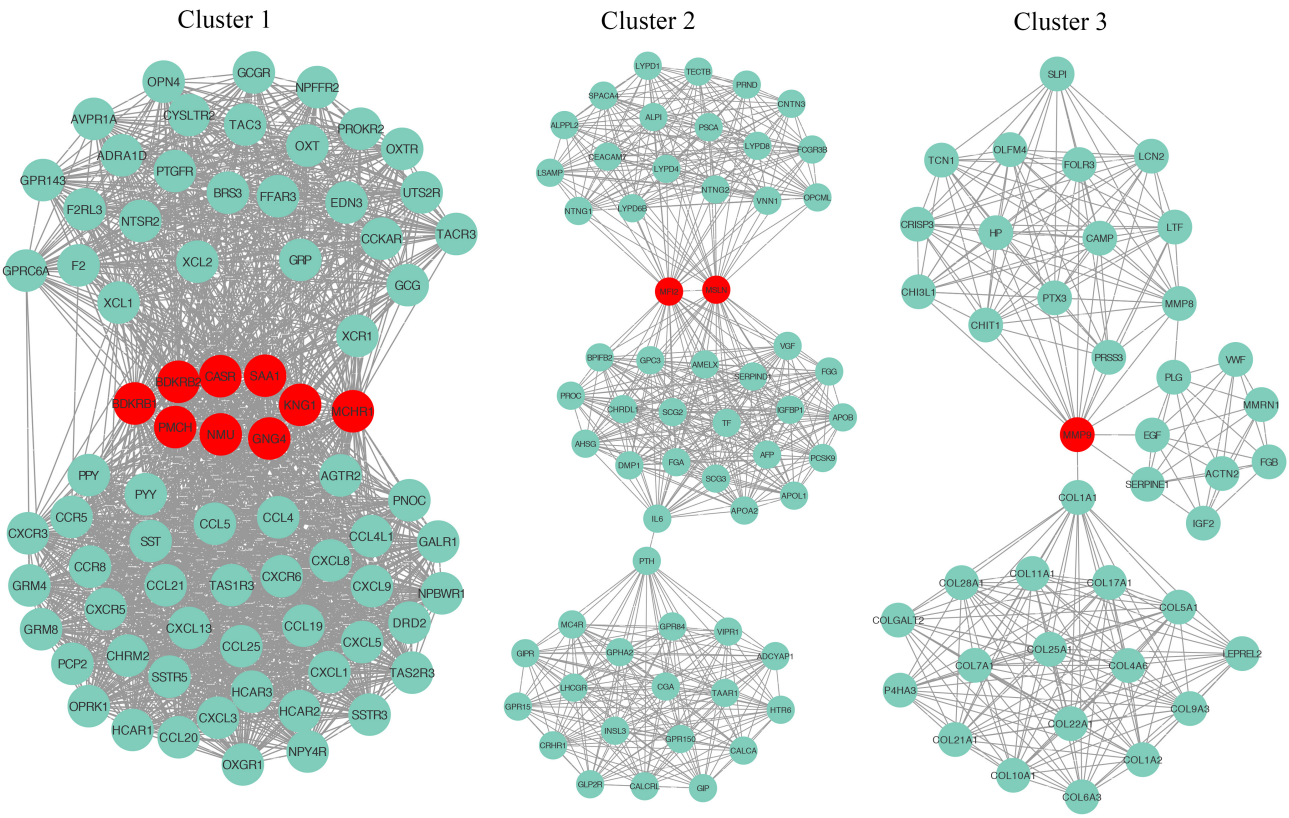

FIGURE 5 | The identification of hub genes. Three gene clusters were identified from the PPI network by the MCODE plugin. The hub genes are highlighted in red dots.

TABLE 2 | List of the 13 hub genes.

Gene	Full name
CASR	Calcium sensing receptor
BDKRB1	Bradykinin receptor B1
MMP9	Matrix metallopeptidase 9
MSLN	Mesothelin
COL1A1	Collagen type I alpha 1 chain
NMU	Neuromedin U
KNG1	Kininogen 1
MCHR1	melanin concentrating hormone receptor 1
MFI2	Melanotransferrin 2
GNG4	G protein subunit gamma 4
BDKRB2	Bradykinin receptor B2
SAA1	Serum amyloid A1
PMCH	Pro-melanin concentrating hormone

Relationship Between Clinical Traits and Survival-Related Immune Cells

We measured the relationship between clinical traits and the abundance ratios of survival-related immune cells. The abundance ratio of regulatory T cells increased with the increase of pathological grades and clinical stages (**Figure 2A**), while the abundance ratio of resting mast cells decreased with the increase of pathological grades and clinical stages (**Figure 2B**). The abundance ratio of memory B cells was statistically different in distinct pathological grades ($p < 0.05$). However, we still suggest that there was no change with the increase of pathological grades since the abundance ratio of memory B cells in most cases was relatively small and the difference probably attributed to the outliers (**Figure 2C**). The abundance ratio of plasma cells slightly increased in pathological grade 4 (**Figure 2D**). The abundance ratios of M0 macrophages, resting dendritic cells, and activated dendritic cells showed no significant difference in distinct grades or stages (**Figures 2E–G**). These results indicate that the abundance ratios of survival-related immune cells are not necessarily related to the pathological grade or clinical stage.

Identification of Immune-Related Genes

We screened the genes related to the abundance ratios of the survival-related immune cells with the method described in the Materials and Methods and found 3863 genes related to the abundance of the seven types of survival-related immune cells. In all these genes, 1325 genes were related to memory B cells, 651 to plasma cells, 1419 to regulatory T cells, 1515 to M0 macrophages, 837 to resting dendritic cells, 1052 to activated dendritic cells, and 1144 to resting mast cells (**Figures 3A–G**). The distribution of immune-related genes is shown in **Figure 3H**.

Pathway Analysis of Immune-Related Genes

We performed KEGG and Reactome pathway enrichment for each group of immune-related genes to explore the biological function of immune-related genes. The results are listed in **Supplementary Tables S1, S2**. The results with gene counts over ten are shown in **Figure 4**. The KEGG pathway enrichment results showed that the immune-related genes were mainly enriched in neuroactive ligand-receptor binding, cytokine-cytokine receptor interaction (**Figure 4A**). The Reactome

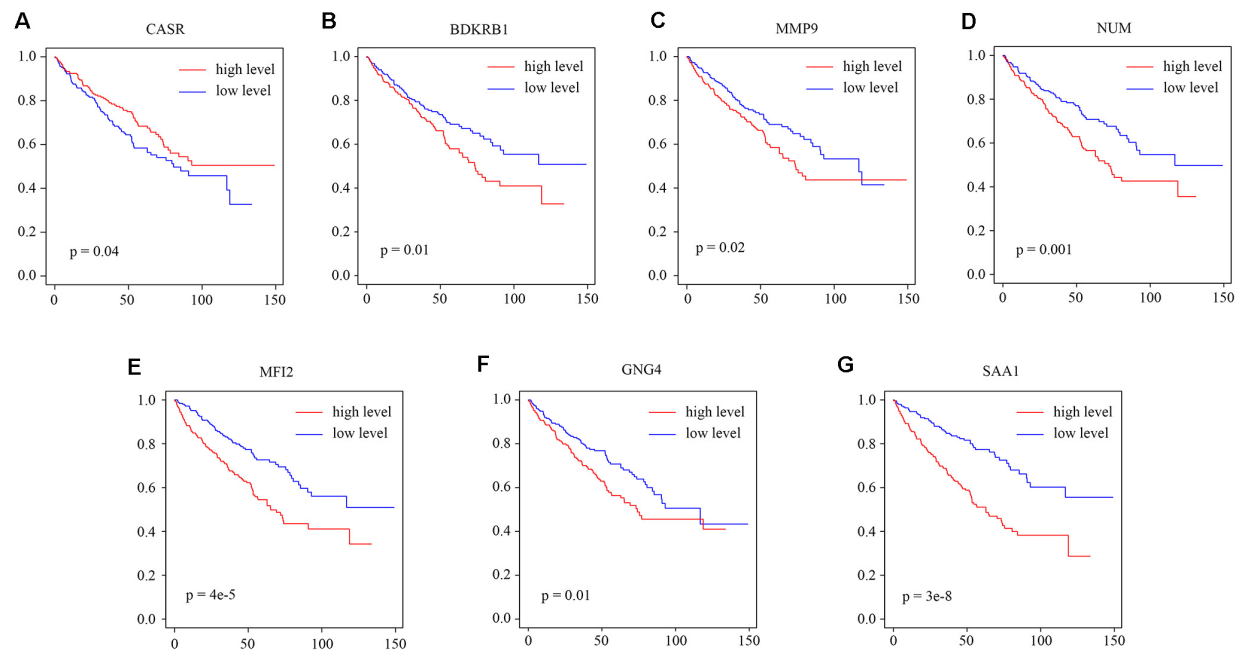

FIGURE 6 | The relationship between the hub genes and overall survival. **(A–G)** The survival analysis for the hub gene CASR, BDKRB1, MMP9, NMU, MFI2, GNG4, and SAA1.

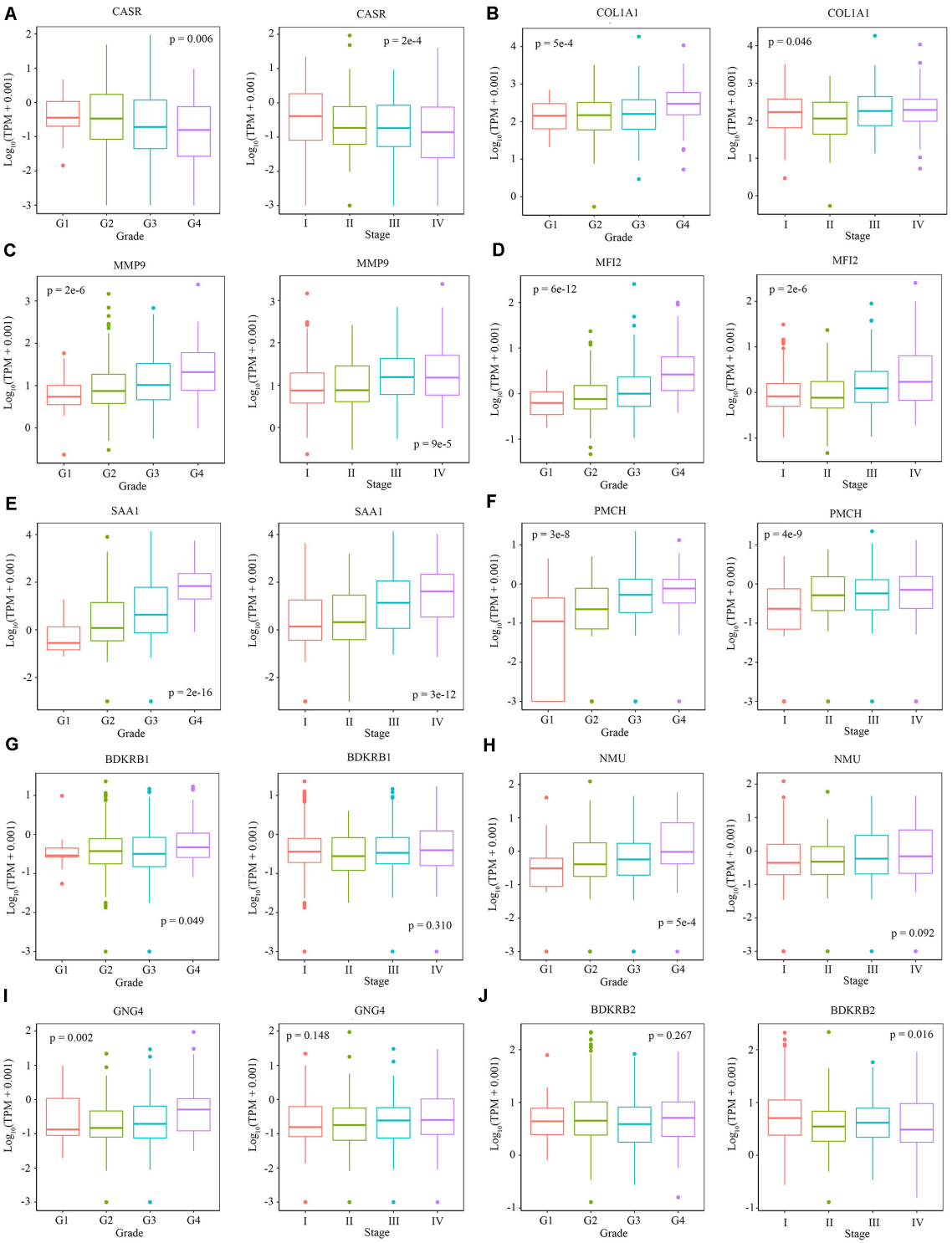

FIGURE 7 | The relationship between the level of hub genes and clinical characteristics. **(A–J)** The level of CARS, COL1A1, MMP9, MFI2, SAA1, PMCH, BDKRB1, NMU, GNG4, and BDKRB2 in different pathological grades and clinical stages. Data are shown in boxplot format, and the dots represent the outliers.

pathways enrichment results showed that the immune-related genes were mainly enriched in G protein-coupled receptor (GPCR) ligand binding, peptide ligand-binding receptors (**Figure 4B**). These results indicate that the immune-related genes might be involved in ligand-receptor binding and signaling pathway transduction.

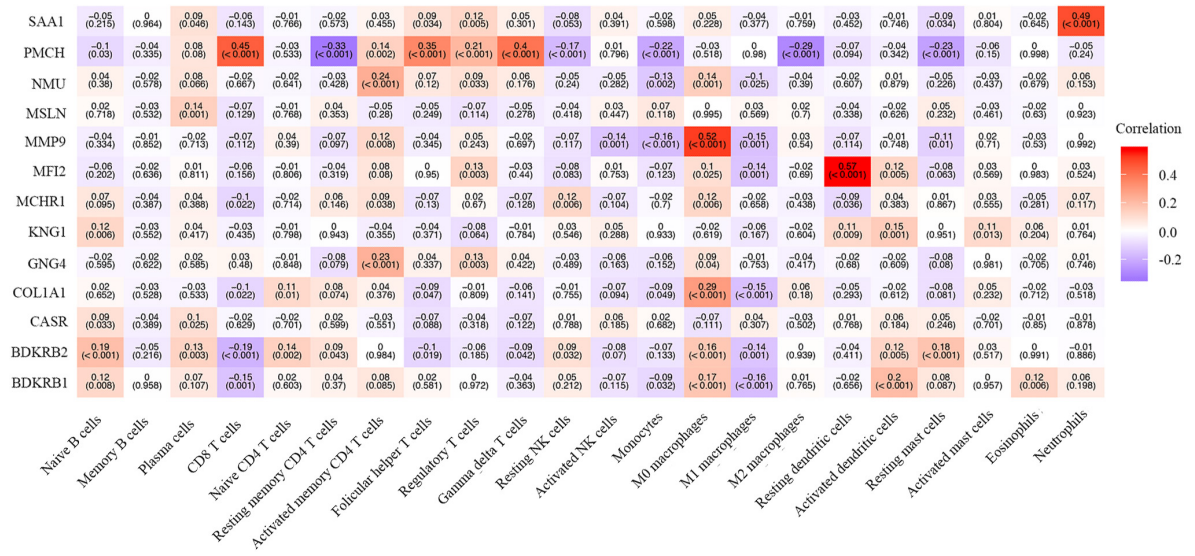

FIGURE 8 | The correlation between the hub genes and immune cells. The Pearson correlation coefficients are presented with a heatmap. The number without brackets is the Pearson correlation coefficients, and the number with brackets is the *p*-value.

Identification of Hub Genes

To explore the detail of immune-related gene relationships, we constructed the PPI with all the protein-coding genes in the immune-related gene set. To identify the critical immune-related gene, we explored the gene clusters within the PPI network with the MCODE plugin of the Cytoscape software. Three clusters with no less than 40 genes were found and applied to identify the hub genes. Here, the Hub genes were those genes with the most interacted genes in the cluster. Finally, 13 genes were identified as the hub genes (**Figure 5** and **Table 2**).

Relationship Between Clinical Traits and Hub Genes

We explored the relationship between the overall survival and the hub genes. We found that 7 out of 13 hub genes (CASR, BDKRB1, MMP9, NMU, MFI2, GNG4, and SAA1) are correlated to overall survival (**Figure 6**). We also explored the relationship between the clinical traits and the hub genes. The level of CASR decreased with the increase of pathological grades and clinical stages (**Figure 7A**). The level of COL1A1 increased in pathological grade 4 but decreased in clinical stage II (**Figure 7B**). Meanwhile, the levels of MMP9, MFI2, SAA1, and PMCH increased with the increase of pathological grades and clinical stages (**Figures 7C–F**). The levels of BDKRB1, NMU, and GNG4 increased only with the increase of pathological grades (**Figures 7G–I**). The level of BDKRB2 decreased with the increase of clinical stages (**Figure 7J**). The levels of MSLN, KNG1, and MCHR1 showed no difference in distinct pathological grades or clinical stages (**Supplementary Figure S1**).

We also explored the correlation between hub genes and the abundance ratios of 22 types of immune cells. We found that multiple hub genes were correlated to the abundance ratio of certain types of immune cells (**Figure 8**). For instance, the level of MMP9 was positively correlated to the abundance ratio of M0 macrophages, while the level of PMCH was negatively correlated to the abundance ratio of resting mast cells. These results indicate that the hub genes might play a vital role in the function of the immune cells.

DISCUSSION

As the comprehensive molecular characterization of ccRCC has been performed (3, 20–23), genetic and epigenetic prognostic markers have been widely studied (24, 25). Since immune cell infiltration has been widely reported in ccRCC (3, 17–20), the prognostic value of the immune-based markers has emerged. Prognostic models based on tumor-associated immune cells and genes have been developed (26–28). In this study, we pursued to expand the range of immune prognostic tools by exploring microenvironment component of ccRCC. We analyzed the ccRCC microenvironment by calculating the abundance ratios of 22 types of immune cells. The results showed a variation of the abundance ratios among distinct patients, which not only supported those previous research but also indicated that the ccRCC microenvironment might be complex.

We found that seven types of survival-related immune cells, including memory B cells, plasma cells, regulatory T cells, M0 macrophages, resting dendritic cells, activated dendritic cells, and resting mast cells, were correlated with overall survival. A previous study has identified ICOS + Treg cells as a prognostic marker in localized ccRCC, which is consistent with our results (29). Also, Eckl et al. analyzed immune cell infiltration of 41 ccRCC samples with flow cytometry and found that patients with a high level of NK cell infiltration had better cancer-specific survival (30). This result is consistent with our results that the higher abundance ratios of resting dendritic cells and activated

dendritic cells identify patients with better prognosis. These research, to a certain extent, indicate that these seven types of immune cells might be predictors for ccRCC prognosis.

The survival-related immune cells in the microenvironment may be the potential therapeutic targets. Several studies demonstrated that macrophages constitute up to 50% of a tumor mass, forming a major component of the tumor microenvironment (31, 32). A widely accepted theory on macrophage subtypes is the plastic modal that macrophages can be activated into classically polarized tumor-suppressive M1 and alternatively polarized tumor-promoting M2 subtypes. M2 macrophages promote ccRCC progression due to their immune-suppressive property (33, 34). Several therapeutic agents targeting macrophages have been developed in recent years (35, 36). According to our data, the abundance ratio of macrophages is over 30% in ccRCC tumors. Therefore, macrophages might be a potential target for ccRCC treatment.

We also screened the immune-related genes and analyzed their biological functions. Most of the immune-related genes were enriched in neuroactive ligand-receptor binding, cytokine-cytokine receptor interaction, GPCR ligand binding, peptide ligand-binding receptors. These results imply that the immune-related genes may be associated with ligand-receptor binding and its downstream signaling pathways that may be potential therapeutic targets. For instance, G protein-coupled receptor 68 (GPR68), a proton-sensing GPCR, plays a vital role in multiple types of tumors (37, 38). Additionally, several immune-related genes were enriched in the interleukin (IL)-17 signaling pathway. IL-17 is mainly produced by Th17 cells, a subtype of T helper cells (39). The activation of IL-17 signaling pathways leads to the overexpression of Chemokines, Cytokines and matrix metallopeptidases (MMPs) through multiple signaling pathways (40).

We also identified 13 hub genes from the immune-related genes and found seven of them (CASR, BDKRB1, MMP9, NMU, MFI2, GNG4, and SAA1) are correlated with overall survival. CASR, a Calcium-sensing receptor, is expressed in the immune cells including macrophages, eosinophils, and monocytes (41–43). Several studies have reported that CASR expression can be induced by multiple cytokines (44, 45). In murine macrophages, the CASR activates the NACHT, LRR, and NLRP3 inflammasome in a cAMP-dependent manner (46). Additionally, MMP9 is a downstream matrix metallopeptidase of the IL-17 signaling pathway. MMP9 promotes metastasis by degrading the extracellular matrix. Ma et al. reported that the level of MMP9 is higher in metastatic ccRCC than in primary ccRCC (47). The level of MMP9 is associated with poor prognosis in ccRCC patients (48). These results indicate that the hub genes may play a key role in the network of immune-related genes.

There are still limitations in our study. First, the analysis of immune-cell infiltration is based on the TCGA dataset and needs to be validated with samples from other sources. Second, the hub genes are identified from PPI networks based on the String database, which needs to be proved by experiment on cell line models. Third, the abundance ratio of memory B cells is zero in most cases, which means the conclusion on memory B cells relays on outliers. Although these results are statistically reliable, we should be cautious with the conclusion on memory B cells. Fourth, intra-tumor heterogeneity of pathological grades in ccRCC has been reported (49). Thus, we need to be cautious about the conclusion on the relation between pathological grades and immune-related cells and genes.

In the past decade, immune checkpoint inhibition therapy has been developed. Nivolumab, a monoclonal antibody targeting programmed death-1 (PD-1), was approved as the second-line treatment for advanced RCC in 2015. Mikami et al. explored the level of PD-1 and programmed death ligand 1 (PD-1L) in tumor-infiltrating immune cells in the tumor microenvironment of untreated and VEGF-TKI-treated primary ccRCC tissues. They found that the high level of PD-1 and PD-L1 in tumor-infiltrating immune cells was associated with the poor prognosis and the clinical response to VEGF-TKI treatment for metastatic ccRCC (50). These results indicate the potential effect of microenvironment on the immune checkpoint inhibition therapy. In conclusion, we identified seven types of survival-related immune cells and 13 hub genes, and seven of these genes were correlated to overall survival in ccRCC patients. These cells and genes can be considered predictors for prognosis, or as therapeutic targets for ccRCC. Our research not only provides a critical understanding of ccRCC microenvironments but also identifies the potential therapeutic targets.

DATA AVAILABILITY STATEMENT

Publicly available datasets were analyzed in this study. This data can be found here: The Cancer Genome Atlas (https://portal.gdc.cancer.gov/).

AUTHOR CONTRIBUTIONS

BD, SX, JD, LQ, HH, and WZ: study concept and design. BD, XY, and TZ: analysis and interpretation of data. BD and YZ: drafting of the manuscript. SX, CT, TS, KZ, and HH: critical revision of the manuscript. All authors contributed to the article and approved the submitted version.

FUNDING

This study was supported by the National Natural Science Foundation of China (No. 81972402) and China Postdoctoral Science Foundation (No. 2019t120970).

SUPPLEMENTARY MATERIAL

The Supplementary Material for this article can be found online at: https://www.frontiersin.org/articles/10.3389/fonc.2020.01770/full#supplementary-material

FIGURE S1 | The relationship between the level of hub genes and clinical characteristics. **(A–C)** The level of MSLN, KNG1 and MCHR1 in different pathological grades and clinical stages. Data are shown in boxplot format, and the dots represent the outliers.

REFERENCES

1. Siegel RL, Miller KD, Jemal A. Cancer statistics, 2020. *CA Cancer J Clin.* (2020) 70:7–30. doi: 10.3322/caac.21590
2. Hsieh JJ, Purdue MP, Signoretti S, Swanton C, Albiges L, Schmidinger M, et al. Renal cell carcinoma. *Nat Rev Dis Prim.* (2017) 3:17009. doi: 10.1038/nrdp.2017.9
3. Ricketts CJ, De Cubas AA, Fan H, Smith CC, Lang M, Reznik E, et al. The cancer genome atlas comprehensive molecular characterization of renal cell carcinoma. *Cell Rep.* (2018) 23:3698. doi: 10.1016/j.celrep.2018.06.032
4. Lopez-Beltran A, Scarpelli M, Montironi R, Kirkali Z. 2004 WHO classification of the renal tumors of the adults. *Eur Urol.* (2006) 49:798–805. doi: 10.1016/j.eururo.2005.11.035
5. Frew IJ, Moch H. A clearer view of the molecular complexity of clear cell renal cell carcinoma. *Ann Rev Pathol.* (2015) 10:263–89. doi: 10.1146/annurev-pathol-012414-040306
6. Barata PC, Rini BI. Treatment of renal cell carcinoma: current status and future directions. *CA Cancer J Clin.* (2017) 67:507–24. doi: 10.3322/caac.21411
7. Qian CN, Huang D, Wondergem B, Teh BT. Complexity of tumor vasculature in clear cell renal cell carcinoma. *Cancer.* (2009) 115(Suppl. 10):2282–9. doi: 10.1002/cncr.24238
8. Shen C, Kaelin WG Jr. The VHL/HIF axis in clear cell renal carcinoma. *Sem Cancer Biol.* (2013) 23:18–25. doi: 10.1016/j.semcancer.2012.06.001
9. Gossage L, Eisen T, Maher ER. VHL, the story of a tumour suppressor gene. *Nat Rev Cancer.* (2015) 15:55–64. doi: 10.1038/nrc3844
10. Atkins MB, Tannir NM. Current and emerging therapies for first-line treatment of metastatic clear cell renal cell carcinoma. *Cancer Treat Rev.* (2018) 70:127–37. doi: 10.1016/j.ctrv.2018.07.009
11. Motzer RJ, Escudier B, McDermott DF, George S, Hammers HJ, Srinivas S, et al. Nivolumab versus everolimus in advanced renal-cell carcinoma. *New Engl J Med.* (2015) 373:1803–13. doi: 10.1056/NEJMoa1510665
12. Soultati A, Stares M, Swanton C, Larkin J, Turajlic S. How should clinicians address intratumour heterogeneity in clear cell renal cell carcinoma? *Curr Opin Urol.* (2015) 25:358–66. doi: 10.1097/MOU.0000000000000204
13. Yuan Y. Spatial heterogeneity in the tumor microenvironment. *Cold Spring Harb Perspect Med.* (2016) 6:26583. doi: 10.1101/cshperspect.a026583
14. Denton AE, Roberts EW, Fearon DT. Stromal cells in the tumor microenvironment. *Adv Exp Med Biol.* (2018) 1060:99–114. doi: 10.1007/978-3-319-78127-3_6
15. Wu T, Dai Y. Tumor microenvironment and therapeutic response. *Cancer Lett.* (2017) 387:61–8. doi: 10.1016/j.canlet.2016.01.043
16. Newman AM, Steen CB, Liu CL, Gentles AJ, Chaudhuri AA, Scherer F, et al. Determining cell type abundance and expression from bulk tissues with digital cytometry. *Nat Biotechnol.* (2019) 37:773–82. doi: 10.1038/s41587-019-0114-2
17. Senbabaoglu Y, Gejman RS, Winer AG, Liu M, Van Allen EM, de Velasco G, et al. Tumor immune microenvironment characterization in clear cell renal cell carcinoma identifies prognostic and immunotherapeutically relevant messenger RNA signatures. *Genome Biol.* (2016) 17:231. doi: 10.1186/s13059-016-1092-z
18. Chevrier S, Levine JH, Zanotelli VRT, Silina K, Schulz D, Bacac M, et al. An Immune atlas of clear cell renal cell carcinoma. *Cell.* (2017) 169:736–49e18. doi: 10.1016/j.cell.2017.04.016
19. Hakimi AA, Voss MH, Kuo F, Sanchez A, Liu M, Nixon BG, et al. Transcriptomic profiling of the tumor microenvironment reveals distinct subgroups of clear cell renal cell cancer: data from a randomized phase iii trial. *Cancer Discover.* (2019) 9:510–25. doi: 10.1158/2159-8290.CD-18-0957
20. Clark DJ, Dhanasekaran SM, Petralia F, Pan J, Song X, Hu Y, et al. Integrated proteogenomic characterization of clear cell renal cell carcinoma. *Cell.* (2019) 179:964–83.e31. doi: 10.1016/j.cell.2019.10.007
21. Cancer Genome Atlas Research Network. Comprehensive molecular characterization of clear cell renal cell carcinoma. *Nature.* (2013) 499:43–9. doi: 10.1038/nature12222
22. Sato Y, Yoshizato T, Shiraishi Y, Maekawa S, Okuno Y, Kamura T, et al. Integrated molecular analysis of clear-cell renal cell carcinoma. *Nat Genet.* (2013) 45:860–7. doi: 10.1038/ng.2699
23. Chen F, Zhang Y, Senbabaoglu Y, Ciriello G, Yang L, Reznik E, et al. Multilevel genomics-based taxonomy of renal cell carcinoma. *Cell Rep.* (2016) 14:2476–89. doi: 10.1016/j.celrep.2016.02.024
24. Liu H, Ye T, Yang X, Lv P, Wu X, Zhou H, et al. A panel of four-lncRNA signature as a potential biomarker for predicting survival in clear cell renal cell carcinoma. *J Cancer.* (2020) 11:4274–83. doi: 10.7150/jca.40421
25. Zhou J, Wang J, Hong B, Ma K, Xie H, Li L, et al. Gene signatures and prognostic values of m6A regulators in clear cell renal cell carcinoma–a retrospective study using TCGA database. *Aging.* (2019) 11:1633–47. doi: 10.18632/aging.101856
26. Geissler K, Fornara P, Lautenschlager C, Holzhausen HJ, Seliger B, Riemann D. Immune signature of tumor infiltrating immune cells in renal cancer. *Oncoimmunology.* (2015) 4:e985082. doi: 10.4161/2162402X.2014.985082
27. Xu WH, Xu Y, Wang J, Wan FN, Wang HK, Cao DL, et al. Prognostic value and immune infiltration of novel signatures in clear cell renal cell carcinoma microenvironment. *Aging.* (2019) 11:6999–7020. doi: 10.18632/aging.102233
28. Ghatalia P, Gordetsky J, Kuo F, Dulaimi E, Cai KQ, Devarajan K, et al. Prognostic impact of immune gene expression signature and tumor infiltrating immune cells in localized clear cell renal cell carcinoma. *J Immunother Cancer.* (2019) 7:139. doi: 10.1186/s40425-019-0621-1
29. Giraldo NA, Becht E, Vano Y, Petitprez F, Lacroix L, Validire P, et al. Tumor-infiltrating and peripheral blood T-cell immunophenotypes predict early relapse in localized clear cell renal cell carcinoma. *Clin Cancer Res.* (2017) 23:4416–28. doi: 10.1158/1078-0432.CCR-16-2848
30. Eckl J, Buchner A, Prinz PU, Riesenberg R, Siegert SI, Kammerer R, et al. Transcript signature predicts tissue NK cell content and defines renal cell carcinoma subgroups independent of TNM staging. *J Mol Med (Berlin Germany).* (2012) 90:55–66. doi: 10.1007/s00109-011-0806-7
31. Van Overmeire E, Laoui D, Keirsse J, Van Ginderachter JA, Sarukhan A. Mechanisms driving macrophage diversity and specialization in distinct tumor microenvironments and parallelisms with other tissues. *Front Immunol.* (2014) 5:127. doi: 10.3389/fimmu.2014.00127
32. Qian BZ, Pollard JW. Macrophage diversity enhances tumor progression and metastasis. *Cell.* (2010) 141:39–51. doi: 10.1016/j.cell.2010.03.014
33. Ginhoux F, Schultze JL, Murray PJ, Ochando J, Biswas SK. New insights into the multidimensional concept of macrophage ontogeny, activation and function. *Nat Immunol.* (2016) 17:34–40. doi: 10.1038/ni.3324
34. Poltavets AS, Vishnyakova PA, Elchaninov AV, Sukhikh GT, Fatkhudinov TK. Macrophage modification strategies for efficient cell therapy. *Cells.* (2020) 9:1535. doi: 10.3390/cells9061535
35. Allavena P, Germano G, Belgiovine C, D'Incalci M, Mantovani A. Trabectedin: a drug from the sea that strikes tumor-associated macrophages. *Oncoimmunology.* (2013) 2:e24614. doi: 10.4161/onci.24614
36. Zhou J, Tang Z, Gao S, Li C, Feng Y, Zhou X. Tumor-associated macrophages: recent insights and therapies. *Front Oncol.* (2020) 10:188. doi: 10.3389/fonc.2020.00188
37. Wiley SZ, Sriram K, Liang W, Chang SE, French R, McCann T, et al. GPR68, a proton-sensing GPCR, mediates interaction of cancer-associated fibroblasts and cancer cells. *FASEB J.* (2018) 32:1170–83. doi: 10.1096/fj.201700834R
38. Wiley SZ, Sriram K, Salmeron C, Insel PA. GPR68: an emerging drug target in cancer. *Int J Mol Sci.* (2019) 20:559. doi: 10.3390/ijms20030559
39. Hemdan NY. Anti-cancer versus cancer-promoting effects of the interleukin-17-producing T helper cells. *Immunol Lett.* (2013) 149:123–33. doi: 10.1016/j.imlet.2012.11.002
40. Li X, Bechara R, Zhao J, McGeachy MJ, Gaffen SL. IL-17 receptor-based signaling and implications for disease. *Nat Immunol.* (2019) 20:1594–602. doi: 10.1038/s41590-019-0514-y
41. Yamaguchi T, Kifor O, Chattopadhyay N, Bai M, Brown EM. Extracellular calcium (Ca2+o)-sensing receptor in a mouse monocyte-macrophage cell line (J774): potential mediator of the actions of Ca2+o on the function of J774 cells. *J Bone Mineral Res.* (1998) 13:1390–7. doi: 10.1359/jbmr.1998.13.9.1390
42. Yarova PL, Stewart AL, Sathish V, Britt RD Jr., Thompson MA, Lowe APP, et al. Calcium-sensing receptor antagonists abrogate airway hyperresponsiveness

and inflammation in allergic asthma. *Sci Trans Med.* (2015) 7:284ra60. doi: 10.1126/scitranslmed.aaa0282
43. Yamaguchi T, Olozak I, Chattopadhyay N, Butters RR, Kifor O, Scadden DT, et al. Expression of extracellular calcium (Ca2+o)-sensing receptor in human peripheral blood monocytes. *Biochem Biophys Res Commun.* (1998) 246:501–6. doi: 10.1006/bbrc.1998.8648
44. Canaff L, Hendy GN. Calcium-sensing receptor gene transcription is up-regulated by the proinflammatory cytokine, interleukin-1beta. Role of the NF-kappaB PATHWAY and kappaB elements. *J Biol Chem.* (2005) 280:14177–88. doi: 10.1074/jbc.M408587200
45. Fetahu IS, Hummel DM, Manhardt T, Aggarwal A, Baumgartner-Parzer S, Kallay E. Regulation of the calcium-sensing receptor expression by 1,25-dihydroxyvitamin D3, interleukin-6, and tumor necrosis factor alpha in colon cancer cells. *J Steroid Biochem Mol Biol.* (2014) 144(Pt A):228–31. doi: 10.1016/j.jsbmb.2013.10.015
46. Lee GS, Subramanian N, Kim AI, Aksentijevich I, Goldbach-Mansky R, Sacks DB, et al. The calcium-sensing receptor regulates the NLRP3 inflammasome through Ca2+ and cAMP. *Nature.* (2012) 492:123–7. doi: 10.1038/nature11588
47. Ma J, Li M, Chai J, Wang K, Li P, Liu Y, et al. Expression of RSK4, CD44 and MMP-9 is upregulated and positively correlated in metastatic ccRCC. *Diagnostic Pathol.* (2020) 15:28. doi: 10.1186/s13000-020-00948-6
48. Niu H, Li F, Wang Q, Ye Z, Chen Q, Lin Y. High expression level of MMP9 is associated with poor prognosis in patients with clear cell renal carcinoma. *PeerJ.* (2018) 6:e5050. doi: 10.7717/peerj.5050
49. Ball MW, Bezerra SM, Gorin MA, Cowan M, Pavlovich CP, Pierorazio PM, et al. Grade heterogeneity in small renal masses: potential implications for renal mass biopsy. *J Urol.* (2015) 193:36–40. doi: 10.1016/j.juro.2014.06.067
50. Mikami S, Mizuno R, Kondo T, Shinohara N, Nonomura N, Ozono S, et al. Clinical significance of programmed death-1 and programmed death-ligand 1 expression in the tumor microenvironment of clear cell renal cell carcinoma. *Cancer Sci.* (2019) 110:1820–8. doi: 10.1111/cas.14019

Conflict of Interest: The authors declare that the research was conducted in the absence of any commercial or financial relationships that could be construed as a potential conflict of interest.